Electronic Supplementary Material (ESI) for Dalton Transactions.

Raman and NMR Spectroscopic and Theoretical Investigations of the Cubic Laves-Phases *RE*Al_2 (*RE* = Sc, Y, La, Yb, Lu)

Elias C. J. Gießelmann, Stefan Engel, Weronika Kostusiak, Yuemei Zhang, Petra Herbeck-Engel, Guido Kickelbick, Oliver Janka*

Elias C. J. Gießelmann, **Stefan Engel, Guido Kickelbick,** Inorganic Solid-State Chemistry, Saarland University, Campus C4.1, 66123 Saarbrücken, Germany.

Yuemei Zhang, Weronika Kostusiak, Department of Chemistry and Physics, Warren Wilson College, Swannanoa, NC, 28778, USA.

Weronika Kostusiak, Department of Chemistry, University of Wroclaw, F. Joliot-Curie 14, 50-383 Wroclaw, Poland.

Petra Herbeck-Engel, INM Leibniz Institute for New Materials, Campus D2.2, 66123 Saarbrücken, Germany.

***Corresponding author: Oliver Janka,** Inorganic Solid-State Chemistry, Saarland University, Campus C4.1, 66123 Saarbrücken, Germany, e-mail: oliver.janka@uni-saarland.de

Powder X-ray diffraction data

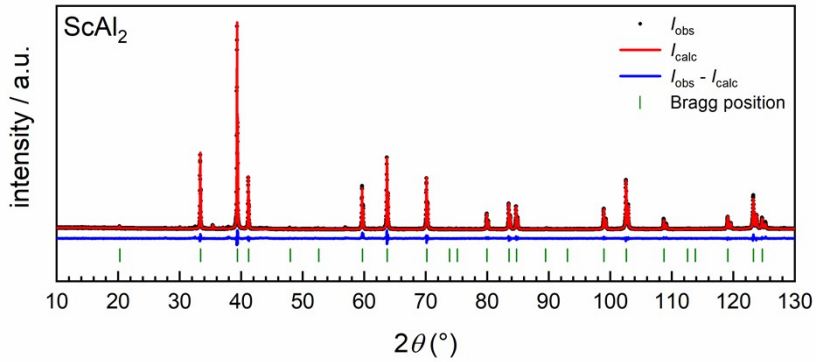

Figure S1. Powder X-ray diffraction data and Rietveld refinement of $ScAl_2$. The black dots represent the experimental data, the red line the respective fit while the blue line indicates the difference between experimental and theoretical data. The green bars show the Bragg positions of cubic $ScAl_2$ ($MgCu_2$ type).

$ScAl_2$ (see Figure S1)	
Source	Bruker D8 ADVANCE (Laboratory X-ray)
Chemical formular	$ScAl_2$
Formula weight / g mol^{-1}	791.3
Temperature	RT
Pressure	ambient
Wavelength / pm	154.0596 and 154.4308
Crystal system	cubic
Space group	$Fd\bar{3}m$ (227)
A / pm	757.98(1)
V / nm^3	0.4355
Z	8
d-space range / Å	0.85-14.35 (6-130° 2θ)
χ^2	1.75
R_p	7.99
R_{wp}	10.56
Definition of R Factors	$R_p = \sum\lvert w\lvert Y_0 - y_c\rvert^2\rvert$; $R_{wp} = \left(\frac{\sum\lvert w\lvert I_0 - I_c\rvert^2\rvert}{\sum\lvert wI_0^2\rvert}\right)^{\frac{1}{2}}$

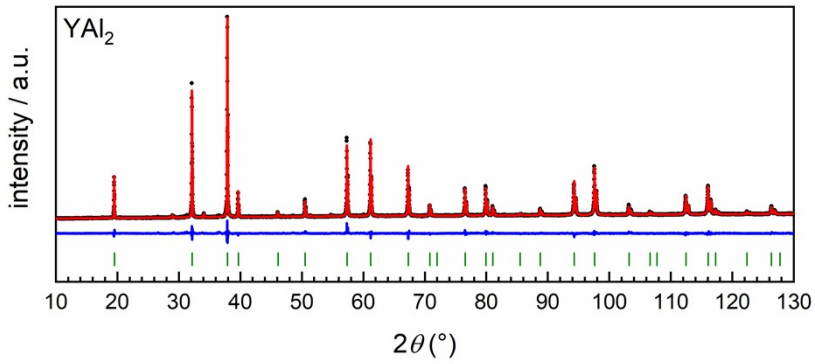

Figure S2. Powder X-ray diffraction data and Rietveld refinement of YAl_2. The black dots represent the experimental data, the red line the respective fit while the blue line indicates the difference between experimental and theoretical data. The green bars show the Bragg positions of cubic YAl_2 ($MgCu_2$ type).

YAl_2 (see Figure S2)	
Source	Bruker D8 ADVANCE (Laboratory X-ray)
Chemical formular	YAl_2
Formula weight / g mol^{-1}	1143.0
Temperature	RT
Pressure	ambient
Wavelength / pm	154.0596 and 154.4308
Crystal system	cubic
Space group	$Fd\bar{3}m$ (227)
A / pm	786.29(1)
V / nm^3	0.4862
Z	8
d-space range / Å	0.85-14.35 (6-130° 2θ)
χ^2	2.56
R_p	3.09
R_{wp}	5.15
Definition of R Factors	$R_p = \sum\|w\|Y_0 - y_c\|^2\|;$ $R_{wp} = \left(\frac{\sum\|w\|I_0 - I_c\|^2\|}{\sum\|wI_0^2\|}\right)^{\frac{1}{2}}$

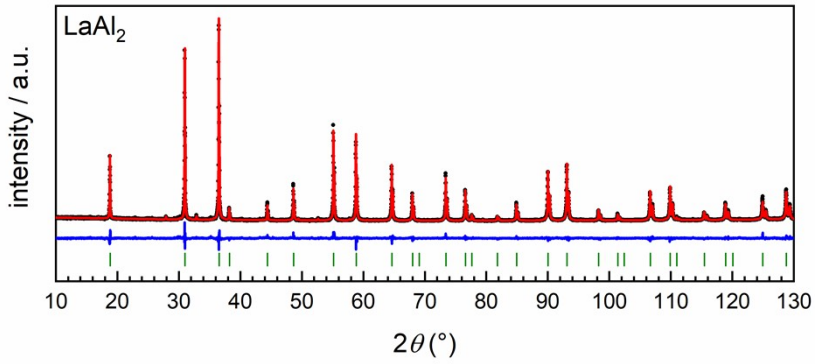

Figure S3. Powder X-ray diffraction data and Rietveld refinement of $LaAl_2$. The black dots represent the experimental data, the red line the respective fit while the blue line indicates the difference between experimental and theoretical data. The green bars show the Bragg positions of cubic $LaAl_2$ ($MgCu_2$ type).

$LaAl_2$ (see Figure S3)	
Source	Bruker D8 ADVANCE (Laboratory X-ray)
Chemical formular	$LaAl_2$
Formula weight / g mol^{-1}	1542.9
Temperature	RT
Pressure	ambient
Wavelength / pm	154.0596 and 154.4308 pm
Crystal system	cubic
Space group	$Fd\bar{3}m$ (227)
A / pm	814.85(1)
V / nm^3	0.5410
Z	8
d-space range / Å	0.85-14.35 (6-130° 2θ)
χ^2	2.63
R_p	9.11
R_{wp}	11.77
Definition of R Factors	$R_p = \sum\lvert w\lvert Y_0 - y_c\rvert^2\rvert$; $R_{wp} = \left(\frac{\sum\lvert w\lvert I_0 - I_c\rvert^2\rvert}{\sum\lvert wI_0^2\rvert}\right)^{\frac{1}{2}}$

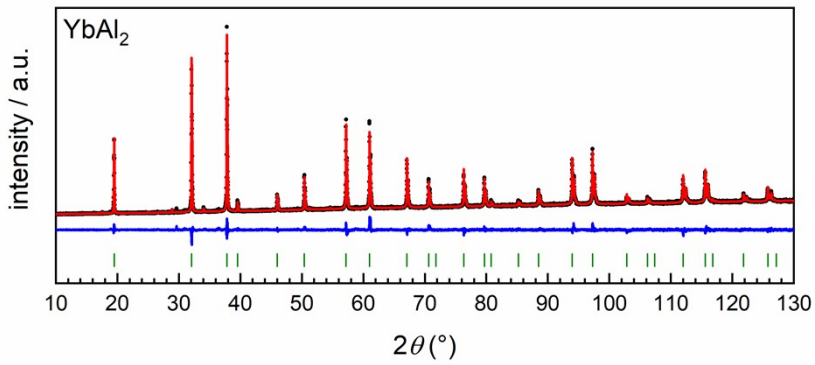

Figure S4. Powder X-ray diffraction data and Rietveld refinement of $YbAl_2$. The black dots represent the experimental data, the red line the respective fit while the blue line indicates the difference between experimental and theoretical data. The green bars show the Bragg positions of cubic $YbAl_2$ ($MgCu_2$ type).

$YbAl_2$ (see Figure S4)	
Source	Bruker D8 ADVANCE (Laboratory X-ray)
Chemical formular	$YbAl_2$
Formula weight / g mol^{-1}	1816.0
Temperature	RT
Pressure	ambient
Wavelength / pm	154.0596 and 154.4308 pm
Crystal system	cubic
Space group	$Fd\bar{3}m$ (227)
A / pm	788.36(1)
V / nm^3	0.4874
Z	8
d-space range / Å	0.85-14.35 (6-130° 2θ)
χ^2	2.17
R_p	3.75
R_{wp}	5.11
Definition of R Factors	$R_p = \sum\|w\|Y_0 - y_c\|^2\|$; $R_{wp} = \left(\frac{\sum\|w\|I_0 - I_c\|^2\|}{\sum\|wI_0^2\|}\right)^{\frac{1}{2}}$

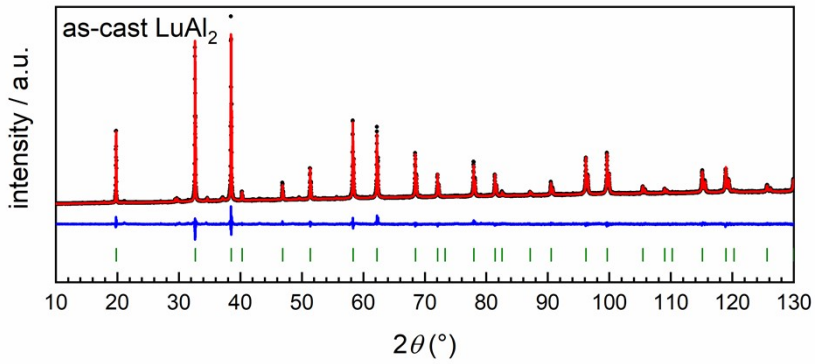

Figure S5. Powder X-ray diffraction data and Rietveld refinement of as-cast $LuAl_2$. The black dots represent the experimental data, the red line the respective fit while the blue line indicates the difference between experimental and theoretical data. The green bars show the Bragg positions of cubic $LuAl_2$ ($MgCu_2$ type).

as-cast $LuAl_2$ (see Figure S5)	
Source	Bruker D8 ADVANCE (Laboratory X-ray)
Chemical formular	$LuAl_2$
Formula weight / g mol^{-1}	1831.4
Temperature	RT
Pressure	ambient
Wavelength / pm	154.0596 and 154.4308 pm
Crystal system	cubic
Space group	$Fd\bar{3}m$ (227)
A / pm	774.37(1)
V / nm^3	0.4643
Z	8
d-space range / Å	0.85-14.35 (6-130° 2θ)
χ^2	2.61
R_p	2.82
R_{wp}	3.94
Definition of R Factors	$R_p = \sum\lvert w\lvert Y_0 - y_c\rvert^2\rvert;$ $R_{wp} = \left(\frac{\sum\lvert w\lvert I_0 - I_c\rvert^2\rvert}{\sum\lvert wI_0^2\rvert}\right)^{\frac{1}{2}}$

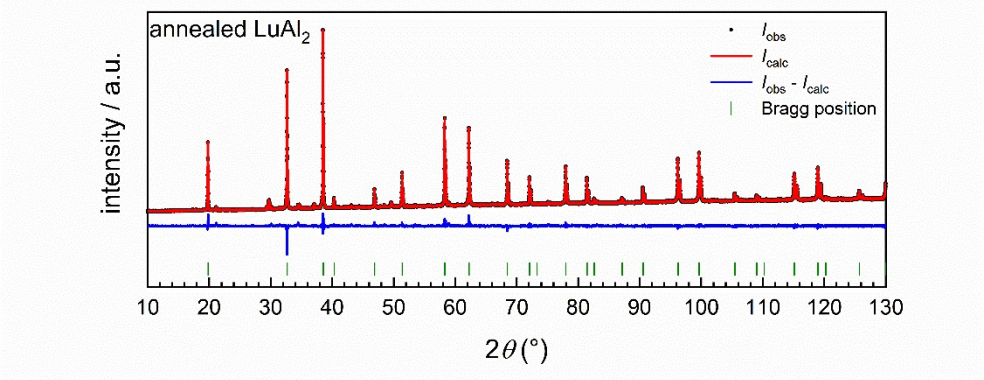

Figure S6. Powder X-ray diffraction data and Rietveld refinement of annealed $LuAl_2$. The black dots represent the experimental data, the red line the respective fit while the blue line indicates the difference between experimental and theoretical data. The green bars show the Bragg positions of cubic $LuAl_2$ ($MgCu_2$ type).

annealed $LuAl_2$ (see Figure S6)	
Source	Bruker D8 ADVANCE (Laboratory X-ray)
Chemical formular	$LuAl_2$
Formula weight / g mol^{-1}	1831.4
Temperature	RT
Pressure	ambient
Wavelength / pm	154.0596 and 154.4308 pm
Crystal system	cubic
Space group	$Fd\bar{3}m$ (227)
A / pm	774.24(1)
V / nm^3	0.4641
Z	8
d-space range / Å	0.85-14.35 (6-130° 2θ)
χ^2	2.89
R_p	3.28
R_{wp}	4.69
Definition of R Factors	$R_p = \sum\lvert w\lvert Y_0 - y_c\rvert^2\rvert;$ $R_{wp} = \left(\frac{\sum\lvert w\lvert I_0 - I_c\rvert^2\rvert}{\sum\lvert wI_0^2\rvert}\right)^{\frac{1}{2}}$

^{27}Al solid state MAS NMR spectroscopy

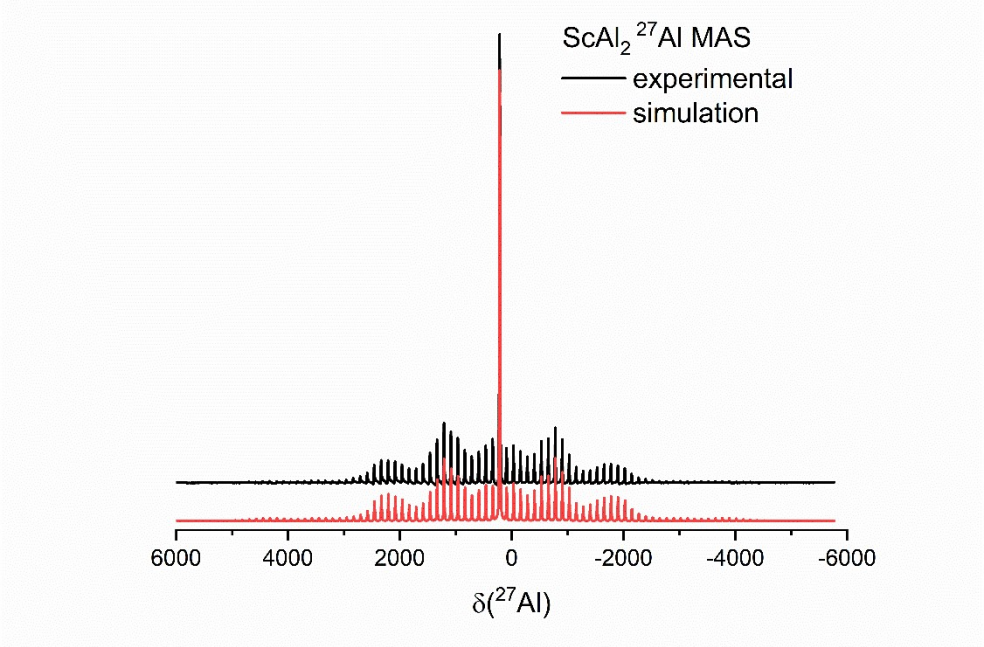

Figure S7. ^{27}Al solid state MAS NMR for cubic $ScAl_2$ ($MgCu_2$ type). The experimental data is shown in black, the fit in red.

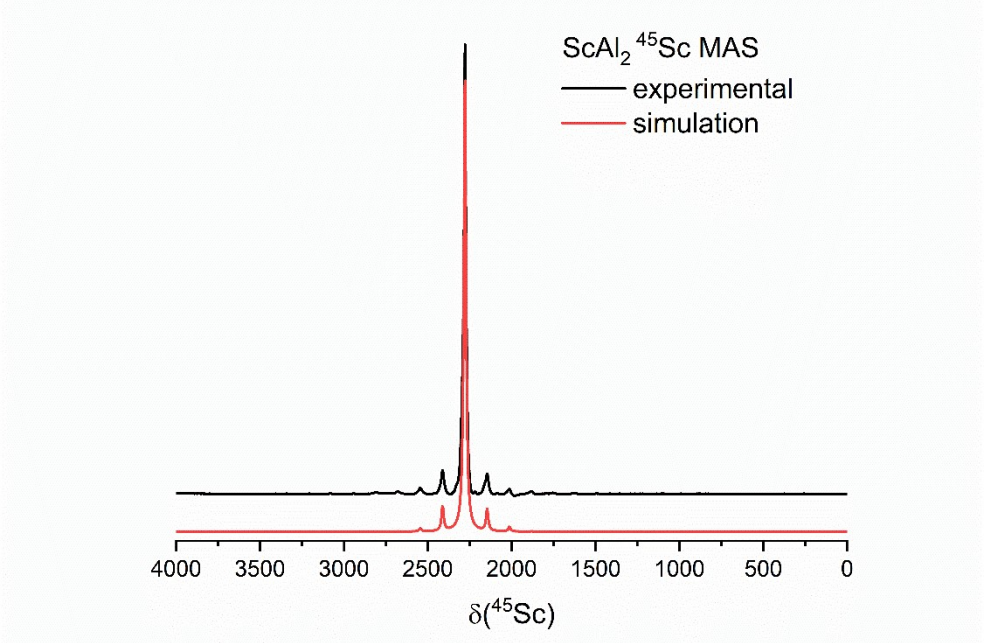

Figure S8. ^{45}Sc solid state MAS NMR for cubic $ScAl_2$ ($MgCu_2$ type). The experimental data is shown in black, the fit in red.

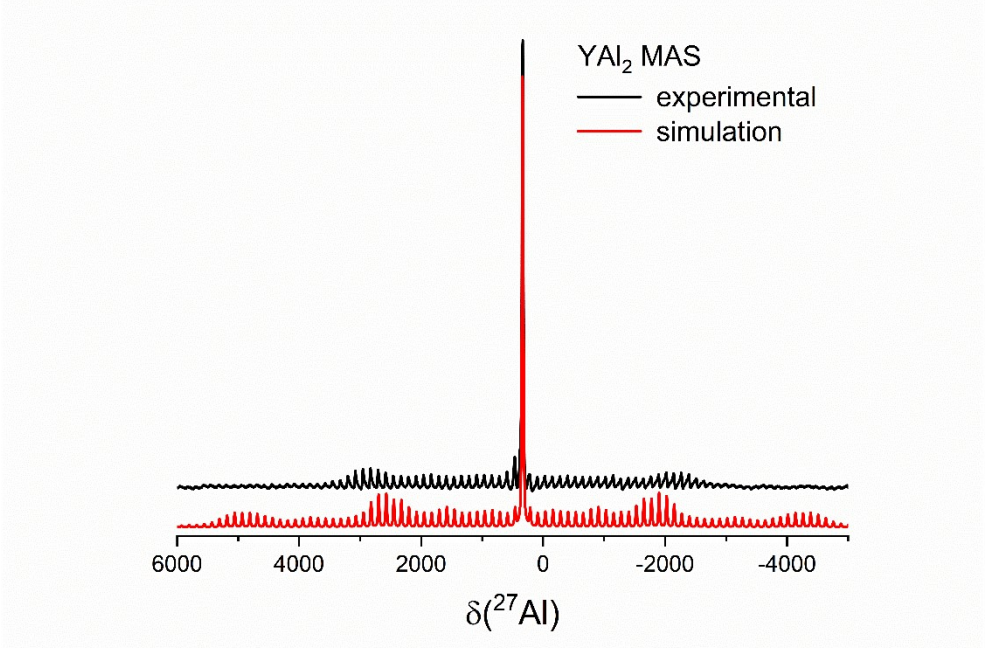

Figure S9. ^{27}Al solid state MAS NMR for cubic YAl_2 ($MgCu_2$ type). The experimental data is shown in black, the fit in red.

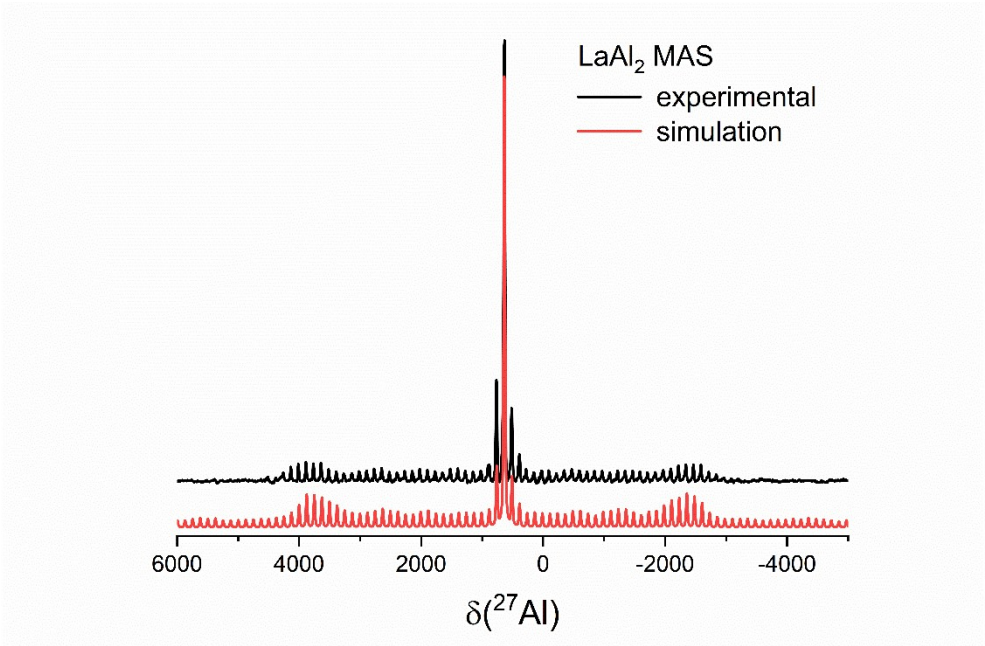

Figure S10. ^{27}Al solid state MAS NMR for cubic $LaAl_2$ ($MgCu_2$ type). The experimental data is shown in black, the fit in red.

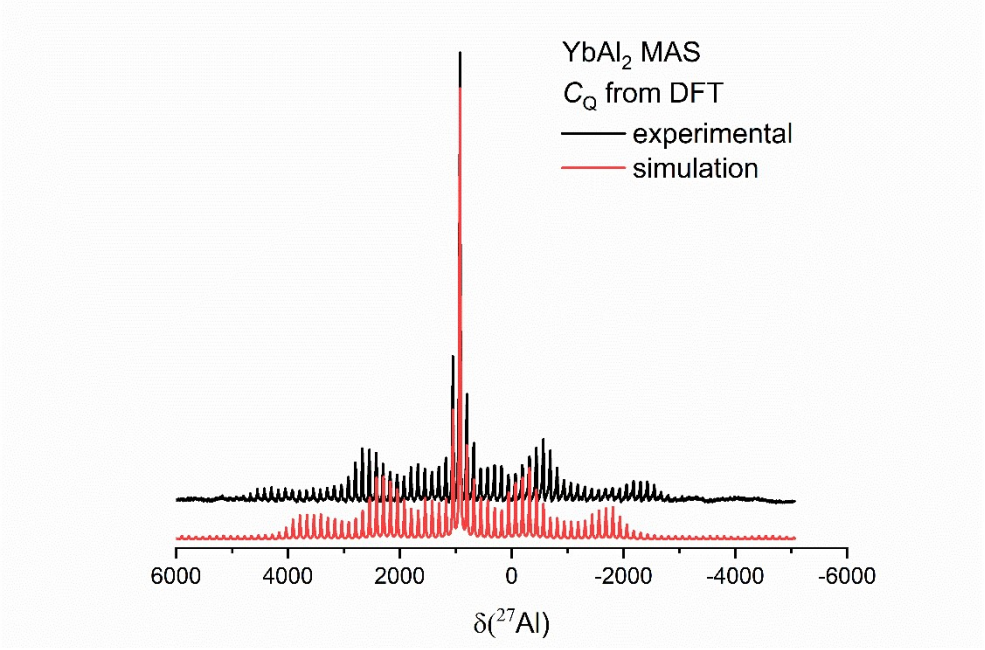

Figure S11. ^{27}Al solid state MAS NMR for cubic $YbAl_2$ ($MgCu_2$ type). The experimental data is shown in black, the fit in red. The C_Q value has been taken from the DFT calculations.

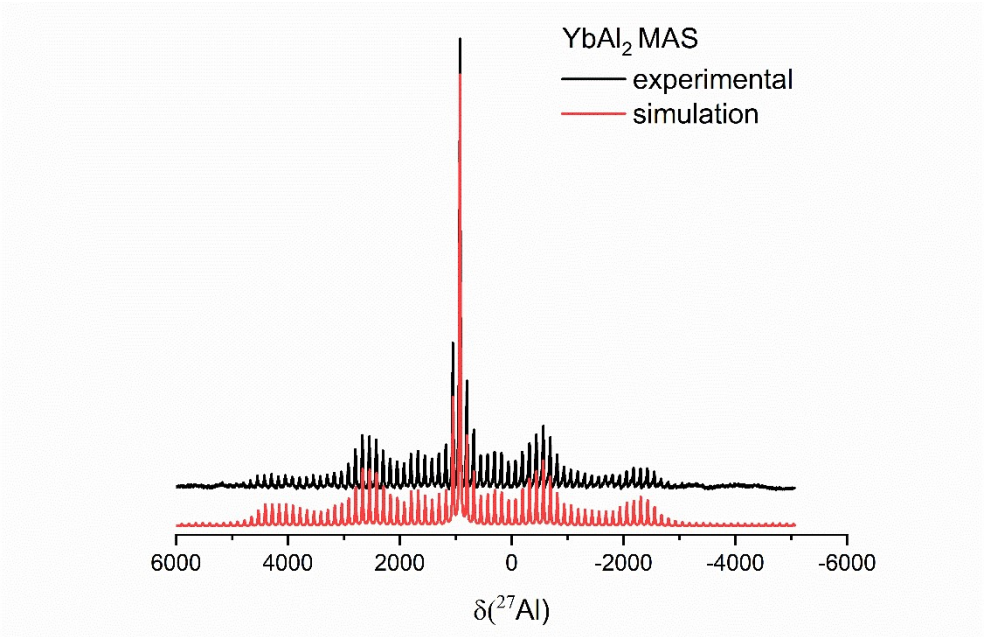

Figure S12. ^{27}Al solid state MAS NMR for cubic $YbAl_2$ ($MgCu_2$ type). The experimental data is shown in black, the fit in red. The C_Q values has been refined.

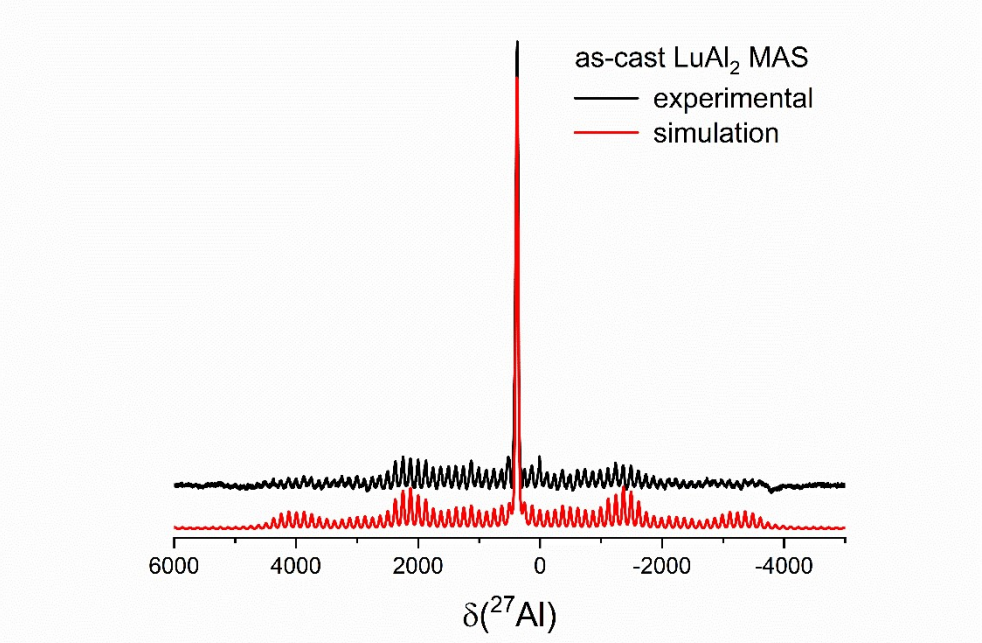

Figure S13. ^{27}Al solid state MAS NMR for as-cast cubic $LuAl_2$ ($MgCu_2$ type). The experimental data is shown in black, the fit in red.

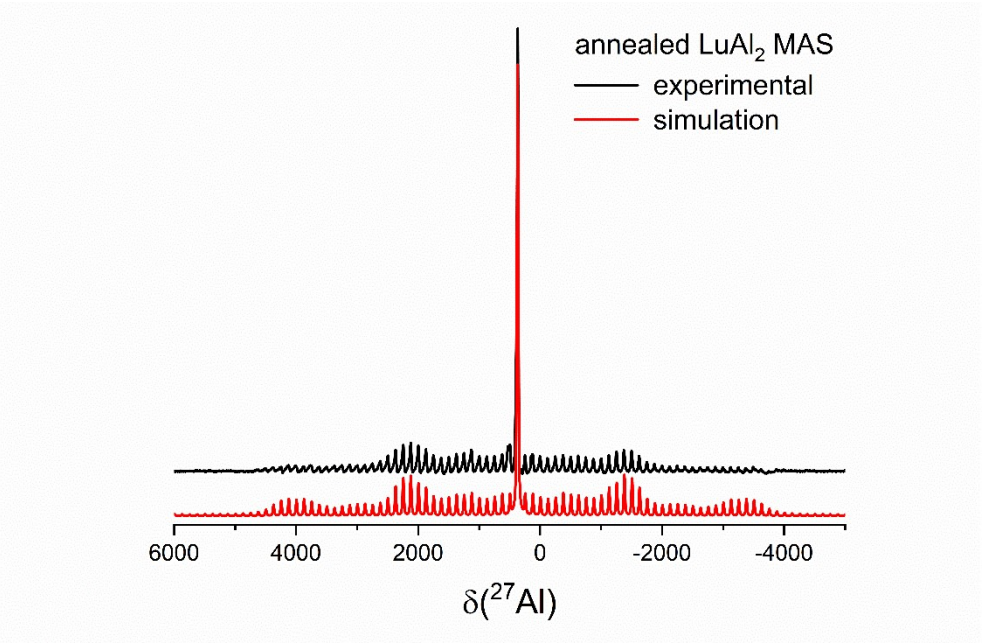

Figure S14. ^{27}Al solid state MAS NMR for annealed cubic $LuAl_2$ ($MgCu_2$ type). The experimental data is shown in black, the fit in red.